

Chapter One

Microscopy of Soft Materials

Eric R. Weeks

Department of Physics, Emory University, Atlanta, GA 30322, USA

I. Introduction

“Soft materials” is a loose term that applies to a wide variety of systems we encounter in our everyday experience, including:

- Colloids, which are microscopic solid particles in a liquid. Examples include toothpaste, paint, and ink.
- Emulsions, which are liquid droplets in another immiscible liquid, for example milk and mayonnaise. Typically a surfactant (soap) molecule or protein is added to prevent the droplets from coalescing.
- Foams, which are air bubbles in a liquid. Shaving cream is a common example.
- Sand, composed of large solid particles in vacuum, air, or a liquid; examples of the latter include quicksand and saturated wet sand at the beach.
- Gels, for example cross-linked polymers such as gelatin, or sticky colloidal particles. Usually the components of a gel (the polymers or particles) are at low concentration, but the gel still is elastic-like due to strong attractive forces between the gel components.

One common feature to all of these materials is that they are all comprised of objects of size 10 nm – 1 mm, that is, objects much larger than atoms. In fact, it is these length scales that gives them their softness, as a typical elastic modulus characterizing these sorts of materials is $k_B T/a^3$, where k_B is Boltzmann’s constant, T is the absolute temperature, and a is the size of the objects the material is made from [1]. For example, a could be the radius of a colloidal particle or of a sand grain, or in a conventional crystalline solid a would be the lattice spacing. For soft materials such as those listed above, a is much larger than the lattice spacing of a crystalline solid, resulting in a much reduced elastic modulus. This then is why soft materials are “soft.”

While grains of sand are large enough to be seen with the naked eye, smaller objects, such as micron-diameter colloidal particles or emulsion droplets, are sufficiently large enough that they are easily viewed with optical microscopy. For this reason, microscopy has become an important tool for studying the structure of these types of samples, for example, how the bubbles in a foam are arranged.

Along with the spatial scales, the temporal scales of these soft systems are often compatible with conventional video microscopy. For example, consider food products such as

mayonnaise or peanut butter. These are somewhat solid-like, in that one can imagine a glob of peanut butter but not a puddle of peanut butter; however, they are also fairly easy to spread with a knife. The speed of spreading with a knife is set by human time scales. For example, a knife moved with velocity $v = 10$ cm/s spreading peanut butter with thickness $h = 4$ mm results in a strain rate given by $\dot{\gamma} = v/h = 25$ s⁻¹. Thus, to understand what happens to the peanut butter microscopically when it is deformed by the knife, one might wish to take 25 images per second, which is easily achieved with inexpensive video cameras that are straightforward to connect to a microscope.

Another relevant time scale is set by diffusion. Very small particles undergo Brownian motion due to thermal fluctuations. The diffusion constant D for a sphere of radius a is given by the Stokes-Einstein-Sutherland formula,

$$D = k_B T / 6\pi\eta a \quad (1)$$

where η is the liquid viscosity [2, 3]. D then can be used to quantify the particle motion as follows. The motion in the x direction is equally likely to be left or right, so the mean displacement $\langle \Delta x \rangle = 0$, where the angle brackets indicate an average over many different particles. However, the mean square displacement will not be zero, but instead will be proportional to the time Δt over which the displacements are measured:

$$\langle \Delta x^2 \rangle = 2D\Delta t; \quad (2)$$

thus a larger value for D results in faster motion. $\langle \Delta x^2 \rangle$ is often called the variance. If you can imagine injecting a tiny blob of dye molecules at a single point, then the expanding cloud of dye has a characteristic size $\sqrt{\langle \Delta x^2 \rangle}$.

Using the mean square displacement, we can estimate the Brownian time scale τ_B as the time a typical particle takes to diffuse its own size as:

$$\tau_B \equiv a^2 / 2D = 3\pi\eta a^3 / k_B T. \quad (3)$$

For a particle of diameter $2a = 1$ μ m in water ($\eta = 1$ mPa·s) at room temperature, $\tau_B \approx 1$ s. Again, this motion is easy to study with a conventional video camera and a microscope. Of course, particles that are 10 times smaller move 1000 times faster, by Equation 3; nonetheless many systems of interest have micron-sized components.

This chapter will discuss several types of optical microscopy, although it will not provide a complete survey of the variety of microscopy techniques; the interested reader should consult Reference [4]. Likewise, several representative applications of microscopy will be presented, although this will not be an exhaustive review; for more comprehensive review articles of the applicability of microscopy to soft matter experiments, see References [5, 6, 7, 8].

II. Video microscopy

Conventional optical microscopes are powerful, highly sophisticated instruments, which are nonetheless straightforward to use [4]. They are common in biology and biochemistry laboratories, and therefore easy to borrow time on if one does not wish to purchase a microscope. For data acquisition, it is simple to attach a camera to the microscope, whether it be a

conventional “snapshot” camera or a CCD video camera. The latter is now more common, and well-suited for studying samples which move or change. The output of the CCD video camera is usually attached to a frame grabber card in a computer, so that data is saved digitally, although a conventional VCR (video cassette recorder) can also be used.

There are several types of optical microscopy, and frequently the same microscope can be used in different ways by making slight modifications. The simplest technique is termed **brightfield microscopy**. Here, the light source is focused by a lens onto the sample, and the objective lens on the other side of the sample collects the light, allowing the user to see an image of the sample, for example the left image in Figure 1. Note that microscopes can be either “upright”, where the objective lens is above the sample and the light source below, or “inverted,” where the situation is reversed. Upright configurations are good for samples that “float,” such as Langmuir-Blodgett films, which are layers of surfactant molecules on the surface of a water bath [9, 10] (see also Chapter Four). Inverted configurations are useful for samples that “sink,” such as suspensions of dense particles. In some cases, inverted microscopes are also useful as the light source can be moved far above the sample and other instrumentation then placed above the objective.

In brightfield microscopy, the image contrast can be due to components in the sample which absorb light (dyes, for example) or variations in the index of refraction of the sample. Variations in refractive index are common, such as between oil and water in an emulsion; both oil and water are transparent, but the differences in index of refraction allow the oil droplets to be seen. A good example of this effect is milk, which is white not because it contains white components, but because the variations in index of refraction between the water and the milk fat scatter light randomly, resulting in a white appearance. A similar argument explains why snow is white, despite the transparency of ice; it is the reflection and refraction at the ice/air interfaces within the snow.

A second common method is **fluorescence microscopy**. Here, short-wavelength light is sent in, typically through the objective. Fluorescent molecules in the sample absorb this light, and radiate slightly longer wavelength (lower energy) light, which is collected through the objective. Special filters and mirrors are used to direct the light appropriately from the light source to the sample, and from the sample to the camera. In particular, a “dichromatic” (or “dichroic”) mirror reflects the excitation light onto the sample, but allows the emitted light to pass through to the camera or microscope eyepiece. The advantage of fluorescence microscopy is that the dye can be placed in specific parts of the sample, such as in the solid particles of a colloidal suspension, or even in the surfactant molecules stabilizing emulsion droplets. This makes it easier to distinguish different sample components.

Fluorescence microscopy has one significant limitation: photobleaching. After dye molecules absorb the excitation light, but before they emit light, they can chemically react with oxygen present in the sample to form a non-fluorescent molecule. This only happens when they are excited, so photobleaching happens in direct proportion to the illumination light (with the limitation that once all the dye molecules are excited, they have reached saturation). Thus a sample can sit stably for a long time in the dark, but the photobleaching starts precisely when the sample is observed, i.e., when the excitation light is turned on. (Although, this only affects the local region illuminated by the microscope.) Photobleaching manifests itself as the image becoming gradually darker. In some cases, photobleaching can be delayed by adding chemicals such as propyl gallate to the sample, which will bind to the free oxygen

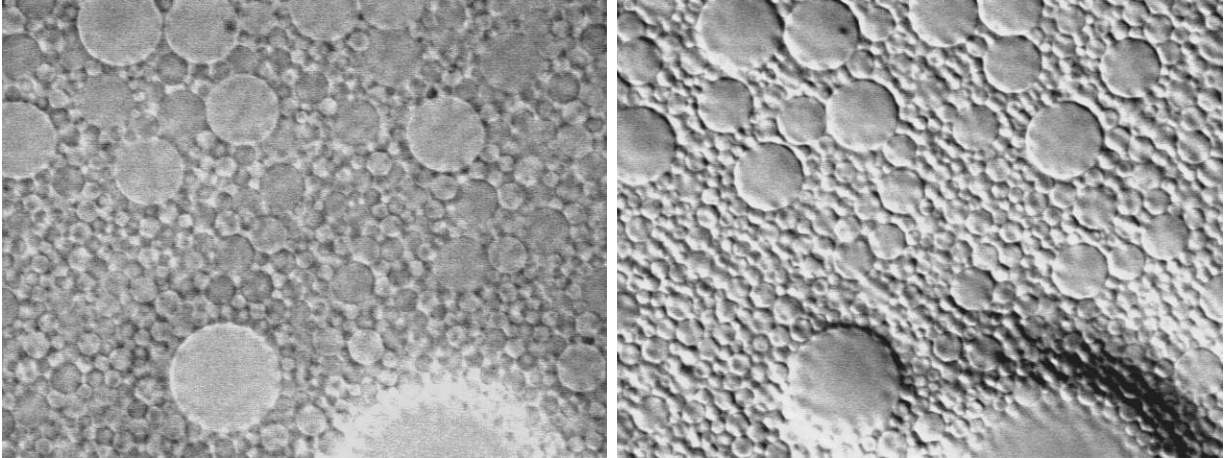


Figure 1: Left: Image of an oil-in-water emulsion taken using brightfield microscopy. The picture is $\sim 60 \mu\text{m}$ wide. Right: Image of the same field of view taken using differential interference contrast microscopy. This form of microscopy produces a fictitious three-dimensional appearance; in reality, these are the cross-sections of spherical droplets. Note: the contrast in both pictures has been enhanced for better appearance.

in the sample. This trick is limited to samples which are compatible with such chemicals, generally restricting the use of these chemicals to non-biological samples. In other cases, photobleaching can be useful for studying local diffusion in samples, a technique known as “fluorescent recovery after photobleaching” [11]. Intense light is used to photobleach a region of the sample, and then low-intensity light is used to monitor the recovery of fluorescence as non-bleached dye molecules diffuse back into the region. With this method, the diffusivity of the dye molecules can be measured.

There are other common types of optical microscopy such as darkfield microscopy, phase contrast microscopy, and differential interference contrast microscopy (see the right image in Figure 1). These are modifications of brightfield microscopy and are able to enhance the contrast from very slight differences in index of refraction. These techniques are more often used in biology, where one might wish to study a cell, filled with water and biopolymers, immersed in a cell culture medium that also is primarily water. These are less often used for soft condensed matter; for more details, see Reference [4].

III. Confocal microscopy

A confocal microscope is a laser scanned optical microscope. This is a fluorescent technique; the laser light is used to excite fluorescence in dye added to a sample. Typically, the laser beam is reflected off two scanning mirrors that raster the beam in the x and y directions on the sample. Any resulting fluorescent light is sent back through the microscope, and becomes descanned by the same mirrors. A dichroic mirror is used to then direct the fluorescent light onto a detector, usually a photomultiplier tube.

One additional modification is necessary to make a confocal microscope: before reaching

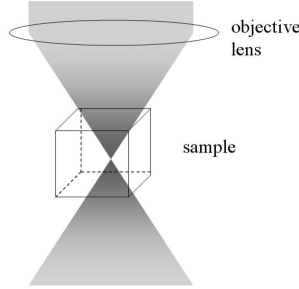


Figure 2: Sketch of light being focused by an objective lens. While the intensity is highest at the focal point, other portions of the sample are illuminated as well.

the detector, the fluorescent light is focused onto a screen with a pinhole. All of the light from the focal point of the microscope passes through the pinhole, while any out of focus fluorescent light is blocked by this screen. This is crucial for viewing samples which may be full of fluorescent objects. Figure 2 shows excitation light being focused through a sample, and clearly the highest intensity of the excitation light is at the focus of the lens. However, the weaker out-of-focus light still excites fluorescence in other layers of the sample. While this emitted light is much weaker (in proportion to the excitation light), there is a large volume where this out-of-focus emitted light emanates. The pinhole filters out most of this out-of-focus light, allowing a strong and clean signal to come from the in-focus region. The pinhole is **conjugate** to the **focal** point of the lens, meaning that a point in focus at the focal point of the objective lens is re-imaged onto the pinhole, and this is the origin of the term “confocal”. Intriguingly, the confocal microscope was invented by Marvin Minsky in 1955, who is much better known for his work in artificial intelligence [12, 13].

This ability to reject out-of-focus fluorescent light directly results in the main strength of confocal microscopy, the ability to take three-dimensional pictures of samples. By rejecting out-of-focus light, a crisp two-dimensional image can be obtained, as shown in Figure 3(a). The sample (or objective lens) can be moved so as to focus at a different height z within the sample, and a new 2D image obtained. By collecting a stack of 2D images at different heights z , a 3D image is built up, as shown in Figure 3(b).

The time to scan one 2D image can range from 10 ms to several seconds, depending on the details of the confocal microscope and the desired image size and quality. For faster rates one typically substitutes an Acoustic-Optical Deflector (“AOD”) for one of the scanning mirrors. This uses a radio-frequency sound wave to set up a standing density wave pattern in a crystal. The standing wave acts as a diffraction grating and steers the laser light depending on the wavelength of the standing wave, which is controlled by the sound wave. Because there are no moving parts, the AOD is faster than a scanning mirror. However, because the diffraction grating behavior is dependent on the wavelength of the diffracted light, the fluorescent light (being a longer wavelength than the excitation light, and not monochromatic) cannot be descanned by the AOD. Thus, AOD-based confocal microscopes replace the confocal pinhole with a confocal slit, with some slight loss of optical performance.

Another high-speed confocal microscopy technique is the Nipkow disk confocal microscope. This uses a spinning disk with many pinholes in it, such that some fraction of the

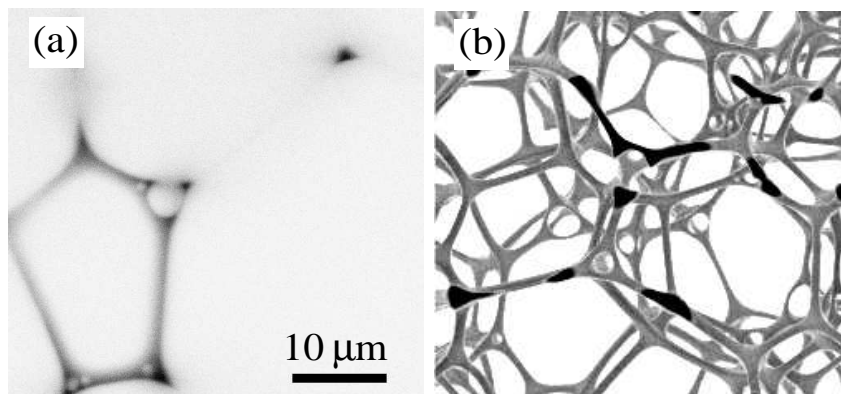


Figure 3: Images from confocal microscopy. (a) a 2D image of a foam. Because of the narrow depth of focus of confocal microscopy, only foam channels that are close to parallel to the field of view are visible. At the upper right, a channel perpendicular to the field of view can be seen as a small black triangle. The depth of focus of this image is approximately $0.5 \mu\text{m}$. (b) 3D image of a foam, $100 \mu\text{m}$ wide. Images from Doug Wise and Eric R. Weeks.

field of view is illuminated at any given moment. As the disk spins, the entire field of view is scanned. The collected light is imaged by a standard video camera rather than a photomultiplier tube, and thus by using different cameras, the technique can be adapted to different conditions (low light levels, higher speed, etc.) Given that there are no moving mirrors, the scanning speed can be quite fast, 100 images/s or more depending on the camera choice. The drawback is that the resolution is not as good, as more out of focus light returns through the pinholes.

IV. Strengths, weaknesses, and tradeoffs

IV.A. Strengths of optical microscopy

Like the other methods described in this book, optical microscopy has strengths and weaknesses. One strength is the ability to visualize heterogeneous structure. Often, complex fluids are spatially heterogeneous (for example, colloidal gels such as the one shown in Figure 4), and it may be desirable to understand this structure. A second strength is the ability to distinguish different features of the material, for example by using fluorescence techniques and adding different dyes to different regions. A third strength is that the data provided by video microscopy is fairly straightforward to understand; directly imaging what is in a sample can often be easier to interpret than more indirect measurements. A fourth strength is the ability to understand local properties. An example of this is studying how granular particles pack next to a wall, and comparing that with the packing in the interior. Other examples will be given in Section VI.

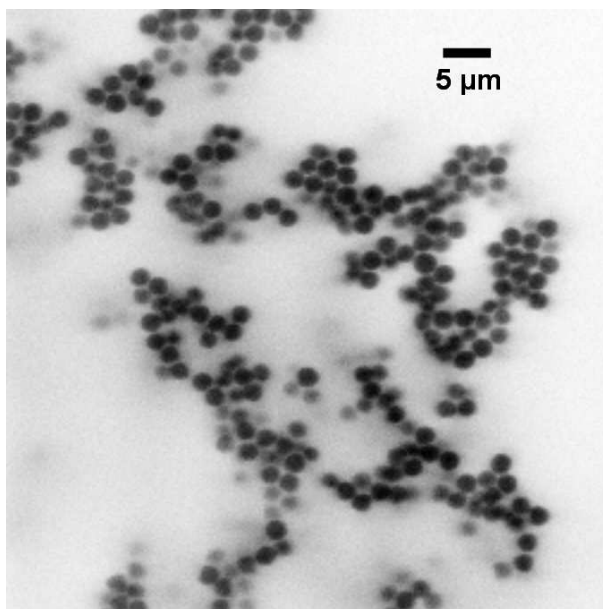


Figure 4: Image of a colloidal gel, taken with confocal microscopy. The particles are $2\ \mu\text{m}$ diameter and aggregate due to the depletion force which is caused by adding small polymers to the solvent [14]. Image from Gary Hunter and Eric R. Weeks. See Chapter Three for more information about colloidal gels.

IV.B. Weaknesses of optical microscopy

A weakness of video microscopy is the necessity to prepare the sample to be compatible with microscopy. Often this means matching the index of refraction of the components. For example, consider a dry sample of small glass spheres, perhaps each $50\ \mu\text{m}$ diameter. These are of the right length scale for microscopy, but each sphere acts like a small lens and scatters light. Thus, this sample will look like white powder, for the same reason as the milk and snow examples discussed above. Microscopy would only be able to see the first layer of particles clearly. To better observe this sample, you would need to add an index-matching fluid. However, then you would be studying a wet sample, and the properties might be much different [15, 16, 17, 18, 19].

A second weakness of video microscopy is the lack of averaging. This shortcoming is complementary to the strength of visualizing spatially heterogeneous structures: while a good picture is gained of the local structure, it might be necessary to examine a large number of different regions to get a true picture of the average structure. For example, consider the case of colloidal crystallization. A sample of monodisperse hard sphere-like colloidal particles can form crystals, usually hexagonal-close-packed, as shown in Figure 5. This occurs at volume fractions $\phi > 0.494$, for reasons due to maximizing entropy by improving the local packing; for a fuller description, see References [1, 20]. Microscopy can be used to study the nucleation of these crystals, but is limited to the crystals that happen to nucleate within the field of view [20, 21]. Direct observation with microscopy can thus determine the specific shapes of a crystal nucleus. On the other hand, a spatially averaging technique like light scattering is

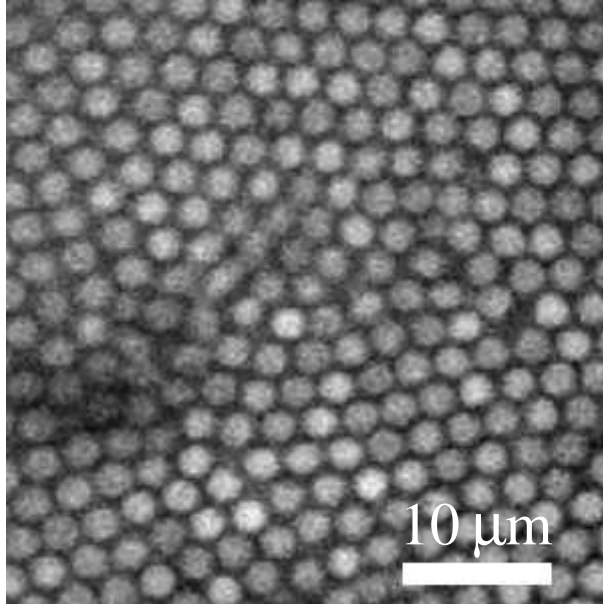


Figure 5: Confocal microscope image of a colloidal crystal. The black patch at the lower left is due to out of focus particles, likely because of a crystalline defect. A grain boundary is seen running through the middle of the image. The particles are $a = 1.18 \mu\text{m}$ and the sample is otherwise similar to those described in Reference [20].

better able to measure the average nucleation rate, but is unable to determine nuclei shapes [22].

IV.C. Tradeoffs when doing optical microscopy

The speed of image acquisition can be either a strength or weakness, depending on the experiment. Video cameras typically acquire images at 30 frames per second (fps). Interlaced video cameras acquire an image alternately from the odd and even rows of pixels, and thus acquire half-images at 60 half-frames per second, which can be useful in some cases [23]. Confocal microscopes, as noted above, have speeds ranging from 1 fps to 30 fps, depending on the hardware. It is possible to use faster cameras, but the tradeoff is then the need to have an illumination level sufficient for the camera. Higher illumination levels (required for faster imaging) will often result in substantial heating of the sample. For fluorescent samples, higher illumination levels cause faster photobleaching.

For confocal microscopy, the main way to achieve faster speeds is to decrease the field of view and number of pixels in the image, so that the scanning optics have shorter distances to cover. One can then maintain the same light levels and the same photobleaching rate as with the slower scanning speed over a larger field of view. It is, of course, harder to take three-dimensional images very quickly; the limitation is how fast the objective can be moved to scan in the z direction. Scanning in the z direction is often achieved by attaching the microscope objective to a fast piezo-electric transducer which is in turn attached to the microscope. In this way 3D images of reasonable size can be acquired at speeds of more than

1 image/s, with faster rates possible for thinner image stacks (thinner in z).

One straightforward tradeoff is the optical resolution as compared to the field of view. Higher magnification lenses have better optical resolution, but at the price of looking at a smaller region within the sample. However, to understand this tradeoff one first needs to understand the relevant terms:

- **Magnification:** Technically this is defined as the apparent angular extent of the image as seen by the eye, compared to the actual angular extent of the object if it was at a reference distance of 25 cm from the eye. In practice, magnification is not a crucial parameter. Any image can be magnified as much as desired by projecting it onto a big screen. Objective lenses typically range from $5\times$ to $100\times$ magnification, and the rest of the microscope optics typically provide an additional factor of $10\times$.
- **Field of view:** More directly useful than the magnification, this is the region within the sample that is viewed. For the highest magnification lenses, the field of view can be as small as $50 \times 50 \mu\text{m}^2$. Field of view also relates to the camera and the optics attaching the camera to the microscope. Typically the field of view as seen by the camera is a quarter of the area seen through the microscope eyepieces.
- **Size of image in pixels:** This depends on the camera. Having more pixels over the same field of view is often helpful, although it requires more room to store the data on a computer. Note, however, that switching to a camera with more pixels does not increase the field of view, which is set by optics. However, the physical size of the CCD chip within a camera can impact the field of view.
- **Resolution:** The optical resolution is set by diffraction effects, quantified by Rayleigh's criterion, and is tied with the quality of the optics and the wavelength of light used to view the sample [4]. The best (smallest) resolution of optical microscopes is about 200 nm. The optical resolution quantifies the ability to distinguish two closely spaced objects. For example, a typical test pattern is a grid of lines, and if the grid spacing is smaller than the resolution, no lines will be seen. Another way to think about resolution is to consider the fluorescence microscopy image of a small fluorescent molecule. The size of the molecule is much smaller than the resolution, but the light emitted from the molecule can still be seen. However, rather than appearing as an extremely sharp point of light, the molecule appears as a fuzzy round spot with a diameter equal to the optical resolution. The best way to think of optical resolution is that all images will be blurry on the scale of the resolution.
- **Ability to resolve features:** Consider the same fluorescent molecule, which appears as a diffraction limited spot. As just mentioned, the presence of this molecule can be detected by the emitted light, and the true size of the molecule is irrelevant (although the intensity of the emitted light may be highly relevant for the ability of the camera to see it). How accurately can the position of the center of this molecule be determined? Perhaps surprisingly, it is easy to do much better than the optical resolution. Suppose the image of the fluorescent molecule spans a region N pixels wide in the image, and each pixel has size δ in microns. Then, typically the position of the molecule can be determined to a precision of $\approx \delta/N$. This argument also holds true for other optical microscopy techniques, not just fluorescence. The real limitation of the resolution is that

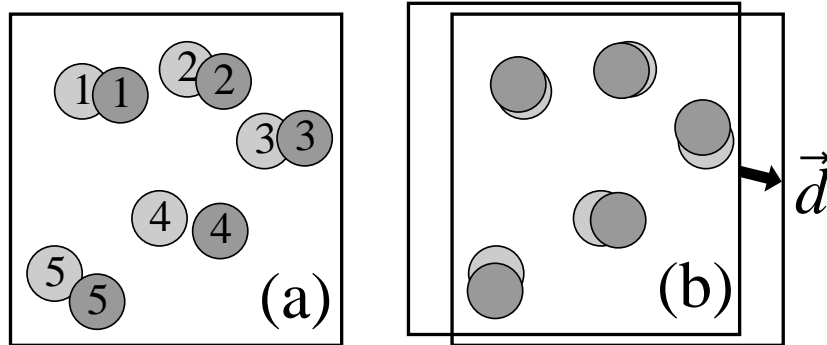


Figure 6: (a) Schematic of particle positions at one time (light gray) and a later time (dark gray). If the particles have not moved much between the two times, particle tracking can assign each particle a unique identity number at each time. (b) In particle image velocimetry, two regions within an image are compared at two different times separated by Δt , and the displacement vector necessary to shift one region onto the other provides the velocity as $\vec{v} = \vec{d}/\Delta t$. This method does not require identifying individual particles, nor does it require that the regions are exact matches, as indicated in this sketch.

two such molecules that are closer together than the resolution will blend together into one diffraction limited spot, and their separation will be nearly impossible to measure. The fact that there are two molecules rather than one might still be measurable by the quantity of emitted light, although this ability applies only to fluorescent techniques.

Overall, as with many experimental techniques, these abilities can be tweaked by spending more money. Higher magnification lenses tend to be more expensive. At a given magnification, lenses with higher resolution are more expensive. In general, the resolution of a lens is reasonably well-suited to the field of view. That is, a high resolution lens with low magnification would not be useful, as then the limitations would be set by the limited pixel size of the camera rather than optical considerations. It is best to work with a camera with pixel sizes at least as small as the resolution of the microscope, that is, an image of an object the size of δ (the resolution limit) should be at least one pixel wide. Without this, you don't get the best abilities of your microscope; you don't want a cheap camera limiting the capability of an expensive microscope.

V. Particle tracking

Particle tracking is a powerful and common technique used to study soft materials [23]. The general idea is to embed tracer particles in your sample that are imaged using video microscopy. By taking a movie of these particles moving, a computer can post-process the images to determine where the particles are at each moment. These particle positions are then used for the tracking step. If the particles do not move large distances between subsequent images, then they can be easily tracked, as shown in Figure 6(a). Specifically, they need to move less between images than their typical inter-particle spacing [23].

In some cases, the particles themselves may be a key part of the sample, for example with colloids or granular materials. With confocal microscopy, particles can be tracked in three dimensions, allowing the structure of the materials to be determined or three-dimensional flow fields to be measured [7, 24]. Specific examples will be discussed in Section VI.

A complementary method is **particle image velocimetry** (PIV). In this method, again a sequence of images is taken. PIV uses the fact that if there is motion within the sample, then small regions within the image will move roughly uniformly between consecutive frames. By identifying how these regions move with time, the coarse-grained displacement can be measured. The key assumption is that the spatial variation of the velocity field is not too great, that is, within a small region the velocity is fairly uniform. Consider two sequentially taken images that are slightly different from each other, and examine a small region of the first image, say 10×10 pixel². To determine the velocity vector, compare this region with nearby 10×10 pixel² regions of the second image. The region from the second image that most closely resembles the region from the first image then indicates that whatever you're looking at has moved to the position of the second region. (If the region in the second image has the same location as the original region, then nothing has moved.) Thus, this measures a displacement vector for the position of the original region, as shown in Figure 6(b). By checking regions everywhere in your picture, you get a displacement vector field. The advantage of this method is that individual particles do not need to be identified. Typically the size of the compared regions are large enough that there are several particles within each region, and so there is enough information within that area to have a sensible determination of where those particles have moved.

One advantage of PIV (compared to particle tracking) is that the particles are never identified as individual particles, and so PIV easily identifies the flow field even for noisy images. This technique works well for samples with good contrast, and is well suited for movies where particles move large distances between images. The advantage of particle tracking is that information is obtained about each and every individual particle, which can be useful in many applications where flow fields aren't the primary interest. Furthermore, with careful techniques that combine PIV and particle tracking, it is possible to track particles even in quickly moving flows where particles move large distances [7]. See Chapter Seven for more information about using particles to measure flow fields.

VI. Specific Applications

This section discusses a few examples of the utility of microscopy for studying soft materials. As noted earlier, these are only representative examples rather than an exhaustive review.

VI.A. Structure of colloidal glasses

A major application of microscopy is to visualize the structure of soft materials. In 1995, van Blaaderen and Wiltzius used a confocal microscope to study the structure of dense colloidal glasses; this study was one of the very first major applications of confocal microscopy to soft materials [25]. To understand their experiment, a few comments about the glass transition should be made.

When some materials are rapidly cooled, they form an amorphous solid known as a glass. The transition from a liquid to a disordered solid is called the glass transition [26, 27]. As the temperature of a molecular glass-forming material is decreased, the viscosity rises smoothly, but rapidly, with little change in the microscopic structure [25, 28, 29]. Colloidal suspensions are a useful model system for studying the glass transition. In particular, colloidal particles can often be considered as hard spheres with an interaction potential due only to excluded volume effects [30, 31]. Hard spheres only interact when their surfaces touch, and then they are strongly repulsive (imagine frictionless marbles, for example). Because of their simplicity, hard spheres are used to simulate properties of crystals, [32, 33], liquids [34, 35, 36], and glasses [37, 38, 39]. Clearly, attractive interactions between atoms and molecules are responsible for dense phases of matter, but given dense states of matter, repulsive interactions play the dominant role in determining the structure [40, 41].

The control parameter for hard sphere systems is the concentration, expressed as the volume fraction ϕ . For $\phi > \phi_g \approx 0.58$ the system acts like a glass. The transition is the point where particles no longer diffuse through the sample; for $\phi < \phi_g$ spheres do diffuse at long times, although the asymptotic diffusion coefficient D_∞ decreases sharply as the concentration increases [28, 39]. The transition at ϕ_g occurs even though the spheres are not completely packed together; in fact, the volume fraction must be increased to $\phi_{\text{RCP}} \approx 0.64$ (for “random-close-packed” spheres [34, 42, 43, 44, 45]) before the spheres are motionless. See Chapters Three and Five for more details of hard sphere systems.

The work of van Blaaderen and Wiltzius studied the structure of colloidal glasses. A key question about glass transitions is whether there is a structural change that explains the increase in viscosity as the glassy state is approached. Indirect measurements suggest there is no change [28, 29]. In their experiment, van Blaaderen and Wiltzius used confocal microscopy to directly observe particle positions in a colloidal glass. Even with full information about particle positions, they did not find any structural change in the glassy state [25]. In particular, they could find no structural correlation length scale, and therefore no direct structural link to the growing viscosity. Several quantities related to structure *could* be measured in their experiments, however, and agreed quite well with simulations of random close packed spheres [25].

This is merely one example of microscopy being used to study the structure of soft materials. Microscopy has also been used to study the structure of colloidal gels [46, 14], colloidal crystals [20, 47, 48], and emulsions [49, 50].

VI.B. Dynamics of colloidal glasses

At the time of the earlier work of van Blaaderen and Wiltzius (1995), confocal microscopy was still a relatively slow technique, taking one second to scan a 2D image and correspondingly longer for a 3D stack of images [46]. The study of colloidal glasses, with their naturally slow dynamics, was thus well-suited to confocal microscopy. Faster microscopy techniques allow the study of faster motion, and in particular, particle tracking techniques enable investigation of how particle motion changes in liquids as the glass transition is approached, rather than only motion within the slower glassy state.

Light scattering techniques allow the measurement of the average behavior of samples. Thus, early light scattering experiments that studied dense colloidal samples found results

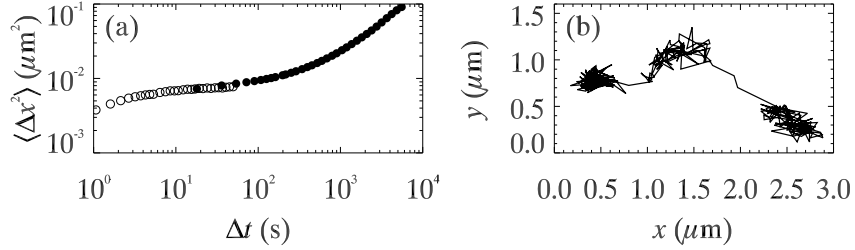


Figure 7: (a) Mean square displacement, measured by confocal microscopy, on a colloidal sample with volume fraction $\phi = 0.52$. Open symbols are from two-dimensional images taken within the 3D sample, and solid symbols are from three-dimensional images of the same sample. The particles in the sample are monodisperse with a radius $a = 1.18 \mu\text{m}$. (b) Particle trajectory from the same sample, showing 120 min of data. The particle started at left, and changed position at $t \approx 51$ min and $t \approx 84$ min. In addition to moving in x and y , the particle also moved $\delta z = 0.3 \mu\text{m}$ during the first jump, and $\delta z = 0.2 \mu\text{m}$ during the second jump.

analogous to the average mean square displacement of particles, as shown in Figure 7. At time scales less than 100 s, particles are “caged” by their neighbors. Because they cannot move past their neighboring particles, the mean square displacement shows a plateau, with the plateau height related to the size of the “cage” formed by the neighbors. At long time scales, particles are able again to diffuse through the sample when the cages rearrange. That is, the neighboring particles somehow rearrange so that the caged particle can move to a new location. Of course, every particle is caged; in other words, not only is a given particle caged, but it also forms part of the cages for its neighbors.

This general picture has been known for a while, and microscopy allows us to directly visualize the motion responsible for cage rearrangements. Figure 7(a) suggests a smooth evolution from diffusion, to cage trapping, to cage rearrangement; perhaps cage rearrangements could be a slow wandering of the position of the particle. Figure 7(b) shows that this is not the case; rather, cage rearrangements can be rather abrupt. The jumps in particle position shown take approximately 1-2 minutes to occur. This is slow compared to a freely diffusing particle, which would diffuse approximately $1 \mu\text{m}$ in 10 s, but fast compared to the time scales between rearrangements in this dense sample. Averaging over thousands of particles which undergo many cage rearrangements results in the smooth curve shown in Figure 7(a).

Furthermore, with microscopy we can answer the question about the motion of the adjacent particles when the cage rearrangement occurs; that is, what does a cage rearrangement look like? Figure 8 shows the motion of several particles in one region. Neighboring particles with large displacements typically move in similar directions, although occasionally cases of neighboring particles with different directions can also be seen [51]. Notably, in general the most mobile particles are clustered together, and also there are regions where particles move relatively little [52, 53]. Overall this is termed “dynamical heterogeneity” – the motion of particles is spatially and temporally heterogeneous. Many experiments provided indirect evidence of dynamical heterogeneity in glassy materials [54], and microscopy allows us to directly see it. While the data shown here are from confocal microscopy, similar results were

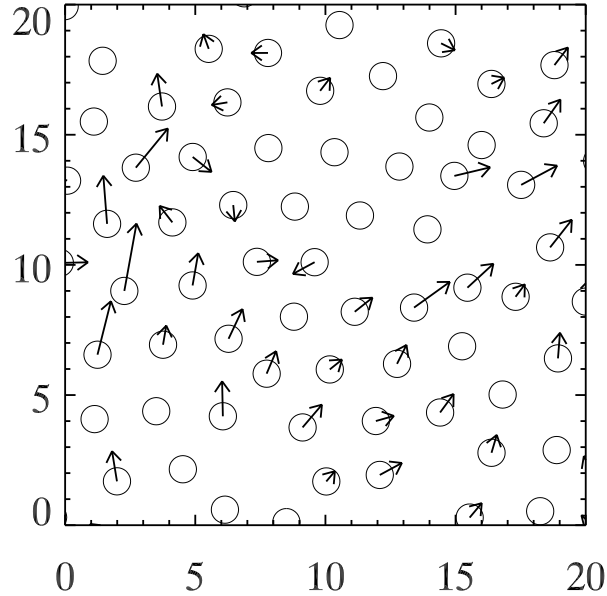


Figure 8: Displacement vectors for particles from the sample shown in Figure 7. The axes are labeled in microns, and the particle radius is $a = 1.18 \mu\text{m}$; the circles indicating particles are not drawn to scale. The time scale for the displacement is 10 min, and the displacement vectors have been stretched by a factor of 5 to make the cooperative motions more apparent. Only particles with displacements longer than $0.1 \mu\text{m}$ are shown. The particles are taken from a $2 \mu\text{m}$ thick slice, and because some have different z positions, they may be closer in x and y than their diameters.

obtained earlier by video microscopy [55, 56].

VI.C. Microrheology: determining macroscopic properties from microscopic measurements

Another widespread application of microscopy is **microrheology**. For example, consider adding a few tracer particles to a Newtonian liquid such as water. Using particle tracking methods, their diffusive motion can be observed and a mean square displacement $\langle \Delta x^2 \rangle (\Delta t)$ calculated. The diffusion constant D can be calculated using Equation 1. If the particle size a and temperature T are known, then the viscosity η of the solvent can be determined from Equation 2. This is the simplest example of microrheology, using the motion of tracer particles to measure the viscosity.

Likewise, consider a particle trapped in a purely elastic medium like gelatin. It too undergoes thermal vibrations, but now the particle is trapped in place. The amplitude of the vibrations is related to $k_B T$ and the elastic modulus of the material. By measuring $\langle \Delta x^2 \rangle (\Delta t \rightarrow \infty)$, the elastic modulus can be determined. More generally, for a viscoelastic material, the Δt dependence of $\langle \Delta x^2 \rangle$ can be used to determine the frequency-dependent viscoelastic moduli [57, 58, 59, 60].

This method is complementary to macroscopic rheology. In a macroscopic rheometer,

a few milliliters of sample are placed in the instrument, for example between two circular plates. In a “controlled strain” rheometer, the top plate is oscillated at a given frequency, and the torque required to maintain that rotation is measured. In a “controlled stress” rheometer, this is reversed: the torque is controlled and the plate displacement is measured. In either case, the relationship between the applied strain and required torque determines the viscoelastic moduli [1, 61]. (In general there is a phase angle between the strain and torque, and the sample has both viscous and elastic moduli. The physical meaning of the phase angle is that the torque and the strain, while both oscillating sinusoidally, do not do so in phase.) A large advantage of microrheology is that the same rheological properties can be measured with *microliters* of sample rather than milliliters. For materials such as biopolymers, purified samples may only be available in tiny quantities. Another advantage is that microrheology can sometimes cover a larger frequency range. Essentially, the camera speed of the microscope sets the highest frequency obtainable, and the duration of the measurement sets the lowest frequency. Using a fast camera, higher frequencies can be studied (> 1000 Hz); macroscopic rheometers typically are limited to about 100 Hz at the fast end. Microrheology can also be done using light scattering techniques, which can get to still higher frequencies [57].

A further advantage of using microscopy for microrheology is that the measurement is local. If the sample is spatially heterogeneous, then this can be observed with microscopy and the local rheology determined. In some cases, microrheology can be used to diagnose spatial heterogeneity. The most straightforward method for this is termed **two-particle microrheology** [62, 63]. This method uses the cross-correlation of the motion of pairs of particles to infer the rheological properties. The cross-correlation can be examined as a function of the separation R of particles. For a homogeneous viscoelastic medium, the correlation should decay as $1/R$. Deviations from this can be used to infer spatial structure of the sample [64]. This method is very robust, and does not depend on the tracer size, shape, or interactions between the tracers and the medium [62]. For example, imagine trying to study microrheology of a polymer network with added tracer particles. The single-particle mean square displacement would be different if particles stick to the polymers, or if the polymers avoid the particles. However, two-particle microrheology will give the correct results in either case, as it only depends on the long-wavelength behavior of the material. The local details which depend on the specific particle/system interactions are uncorrelated over the longer distances, and thus drop out of the analysis.

A limitation of microrheology is that for very stiff or very viscous materials, the particle motion may be hard to observe. For purely viscous materials, $\langle \Delta x^2 \rangle \sim \Delta t / \eta a$, and for purely elastic materials, $\langle \Delta x^2 \rangle \sim 1 / Ga$ (using the elastic modulus G). Thus, for very stiff or very viscous materials, either the particle size a needs to be decreased or else one must be able to measure very small displacements Δx . A limitation of the two-particle method is that, in very spatially heterogeneous samples, one must study the correlated motion of particles separated by distances larger than any spatial heterogeneity, and at those separations, the amount of correlated motion may be very hard to distinguish from the uncorrelated Brownian motion. (Note that macroscopic rheometers avoid this problem by having a macroscopically large gap between the two plates. Samples which are heterogeneous on the scale of a macroscopic rheometer will still have problems, for example, rheology of granular materials is tricky [61].)

See Chapter Six for more details about rheology and microrheology.

VI.D. Flow fields

A final application of microscopy is to determine the flow fields within microscopic samples and microfluidic devices. As mentioned in Section V., this can be done either with particle tracking or particle image velocimetry.

In microscopic systems, the Reynolds number characterizing flow is typically very small. The Reynolds number, given by

$$\text{Re} = UL\rho/\eta, \quad (4)$$

is based on a characteristic velocity U , characteristic length L , viscosity η , and fluid density ρ . So, for water flowing with a maximum velocity of $1000 \mu\text{m/s}$ in a cylindrical tube of radius $100 \mu\text{m}$, $\text{Re} = 0.1$. The Reynolds number indicates the relative importance of inertial and viscous forces. Viscous forces are much more significant in situations with $\text{Re} \ll 1$. For a cylindrical tube, one expects the velocity profile to be parabolic with a zero velocity at the walls (due to the no-slip boundary condition) and maximal velocity along the long axis of the tube. This simple flow field is termed “pipe Poiseuille flow” [65]. Given that microscopes study things at small length scales corresponding to low Reynolds numbers, and flow fields at low Reynolds numbers are simple, why would one want to measure flow fields in microscopic devices? Here we consider three examples where measurements are indeed useful.

Experiments by Frank, *et al.* examined the flow of particle-laden suspensions flowing through rectangular capillary tubes [66]. Indeed, to first approximation, the flow was parabolic in accordance with pipe Poiseuille flow. However, due to shear forces between particles, the particle concentration evolves such that more particles are in the center of the tube compared to near the walls. This is because of the parabolic velocity profile, which ensures that particles move at different velocities. A particle will overtake slower particles which are closer to the wall, and be overtaken by faster particles which are closer to the center of the tube. When two particles moving at different velocities approach each other, they interact via the fluid, which jostles them into new positions. There is an effective diffusivity for this particle which depends on the shear rate, that is, the slope of the velocity gradient. Particles in the center of the tube see a much smaller velocity gradient (since they are at the local maximum of the flow) and tend to stay in the center of the tube. The overall result is that particles move out of regions of high shear (near the walls) and into regions of low shear (in the center) (although note that the full explanation of this phenomenon is more detailed as discussed in Reference [66]). Ultimately for small colloidal particles, this is balanced by diffusion which attempts to homogenize the particle distribution [66]. The heterogeneous particle distribution modifies the velocity profile. Microscopy allows simultaneous measurements of the concentration and velocity profile, and in fact the deviations from a pure parabolic velocity profile agree well with theoretical predictions [66].

The second example relates to mixing in microfluidic devices. In macroscopic applications, turbulence is often used to provide rapid mixing. In microfluidic applications, $\text{Re} \ll 1$, so turbulence is suppressed. Experiments by Gao, *et al.* studied mixing in microfluidic flow chambers designed to enhance mixing [67]. The microchannels had a rectangular cross-section, with occasional raised ridges on the bottom of the channel. The ridges had a “herringbone” pattern, shaped like a “V” with the pointed end of the V pointed downstream. Using confocal microscopy, they studied the flow of moderately concentrated colloidal suspensions through these microchannels. Their observations enabled them to determine the

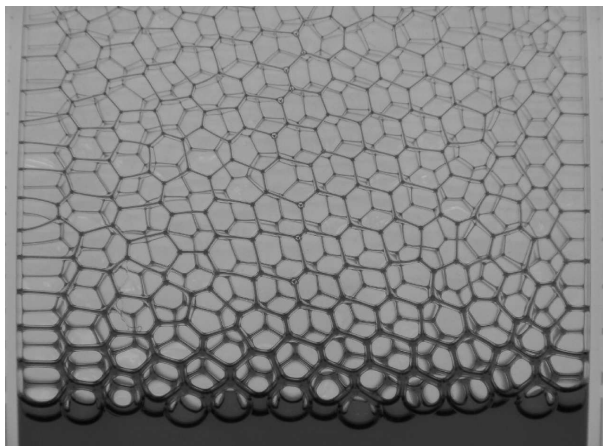


Figure 9: Image of a draining foam. (Taken by Gianguido C. Cianci and Eric R. Weeks.)

best geometries to optimize mixing.

The third example is that of water draining through a foam. Between pairs of bubbles in a foam, one has a foam face. Where three bubbles meet, there is a liquid channel in between; these are visible in Figure 3. Between four mutually adjacent bubbles, four liquid channels come together and meet in a node. Thus the structure of channels and nodes form a network, somewhat like connected pipes, through which liquid can drain out of a foam. Figure 9 shows such a draining foam, and clearly the channels are thicker at the bottom where the liquid has not yet completely drained. Several questions then arise: Are the walls of the bubbles slippery or rigid? Does water flow through the channels like pipe Poiseuille flow, or do the surfactants at the boundaries of the channels prevent a no-slip boundary condition?

Using confocal microscopy, Koehler, *et al.* studied the flow of water through a draining foam [68, 69]. They added water with a few tracer particles at the top of a foam, and by tilting the microscope sideways, were able to study the flow of the water through the foam channels. Foams made with a small-molecule surfactant resulted in plug-like flow, indicating that the channel walls were indeed slippery. For plug-like flow, the velocity is nearly constant across the width of the channel (similar to how toothpaste comes out of the tube). Using a larger protein as a surfactant, they found parabolic flow, indicating that the no-slip boundary condition was recovered. Thus, changing the surfactant can dramatically change the character of foam drainage (and thus the rate at which foams drain).

VII. Summary

Microscopy as a scientific technique dates back many centuries; for example, to the important work of Antonie van Leeuwenhoek in the late 1600's. This book chapter has only touched on suggestive applications of microscopic techniques, and only a few varieties of optical microscopy. Overall, microscopes coupled with video cameras, which in turn can be directly connected to a computer, have greatly expanded the applications of microscopy. Within the

limitations of Section IV., microscopy is a powerful tool for studying soft condensed matter systems. Given that you get to see the samples, it is also a fun technique, as hopefully the images in this chapter have suggested.

VIII. Acknowledgments

I thank J. C. Crocker for helpful discussions on microscopy and particle tracking over many years, and D. Chen, K. W. Desmond, L. Golick, and G. L. Hunter for useful comments on this chapter. This work was supported by the National Science Foundation under Grant No. DMR-0804174.

IX. References

- [1] R. A. L. Jones, *Soft Condensed Matter* (Oxford University Press, USA) (2002), ISBN 0198505892.
- [2] A. Einstein, “On the movement of small particles suspended in a stationary liquid demanded by the molecular-kinetic theory of heat,” *Annalen der Physik (Leipzig)* **17**, 549–560 (1905).
- [3] W. Sutherland, “A dynamical theory of diffusion for non-electrolytes and the molecular mass of albumin,” *Phil. Mag.* **9**, 781–785 (1905).
- [4] S. Inoué and K. R. Spring, *Video Microscopy : The Fundamentals (The Language of Science)* (Springer), 2nd edition (1997), ISBN 0306455315.
- [5] P. Habdas and E. R. Weeks, “Video microscopy of colloidal suspensions and colloidal crystals,” *Current Opinion in Colloid & Interface Science* **7**, 196–203 (2002).
- [6] V. Prasad, D. Semwogerere, and E. R. Weeks, “Confocal microscopy of colloids,” *J. Phys.: Cond. Matt.* **19**, 113102 (2007).
- [7] R. Besseling, L. Isa, E. R. Weeks, and W. C. K. Poon, “Quantitative imaging of colloidal flows,” *Advances in Colloid and Interface Science* **146**, 1–17 (2009).
- [8] V. J. Anderson and H. N. Lekkerkerker, “Insights into phase transition kinetics from colloid science,” *Nature* **416**, 811–815 (2002).
- [9] M. Sickert, F. Rondelez, and H. A. Stone, “Single-particle brownian dynamics for characterizing the rheology of fluid langmuir monolayers,” *Europhys. Lett.* **79**, 66005 (2007).
- [10] R. Walder, C. F. Schmidt, and M. Dennin, “Combined macro- and microrheometer for use with langmuir monolayers,” *Rev. Sci. Inst.* **79**, 063905 (2008).
- [11] D. Axelrod, D. Koppel, J. Schlessinger, E. Elson, and W. Webb, “Mobility measurement by analysis of fluorescence photobleaching recovery kinetics,” *Biophys. J.* **16**, 1055–1069 (1976).

- [12] M. Minsky, “Memoir on inventing the confocal scanning microscope,” *Scanning* **10**, 128–138 (1988).
- [13] M. Minsky, “Memoir on inventing the confocal scanning microscope,” <http://web.media.mit.edu/~minsky/papers/ConfocalMemoir.html> (1988).
- [14] A. D. Dinsmore, V. Prasad, I. Y. Wong, and D. A. Weitz, “Microscopic structure and elasticity of weakly aggregated colloidal gels,” *Phys. Rev. Lett.* **96**, 185502 (2006).
- [15] R. A. Bagnold, “Experiments on a gravity-free dispersion of large solid spheres in a Newtonian fluid under shear,” *Proc. Roy. Soc. London. Series A.* **225**, 49–63 (1954).
- [16] A. Samadani and A. Kudrolli, “Segregation transitions in wet granular matter,” *Phys. Rev. Lett.* **85**, 5102–5105 (2000).
- [17] N. Jain, D. V. Khakhar, R. M. Lueptow, and J. M. Ottino, “Self-organization in granular slurries,” *Phys. Rev. Lett.* **86**, 3771–3774 (2001).
- [18] J. C. Géminard, W. Losert, and J. P. Gollub, “Frictional mechanics of wet granular material,” *Phys. Rev. E* **59**, 5881–5890 (1999).
- [19] H. A. Barnes, “Shear-thickening (‘dilatancy’) in suspensions of nonaggregating solid particles dispersed in Newtonian liquids,” *J. Rheo.* **33**, 329–366 (1989).
- [20] U. Gasser, E. R. Weeks, A. Schofield, P. N. Pusey, and D. A. Weitz, “Real-space imaging of nucleation and growth in colloidal crystallization,” *Science* **292**, 258–262 (2001).
- [21] P. Wette, H. J. Schöpe, and T. Palberg, “Microscopic investigations of homogeneous nucleation in charged sphere suspensions,” *J. Chem. Phys.* **123**, 174902 (2005).
- [22] P. Wette, H. J. Schöpe, and T. Palberg, “Crystallization in charged two-component suspensions,” *J. Chem. Phys.* **122**, 144901 (2005).
- [23] J. C. Crocker and D. G. Grier, “Methods of digital video microscopy for colloidal studies,” *J. Colloid Interf. Sci.* **179**, 298–310 (1996).
- [24] A. D. Dinsmore, E. R. Weeks, V. Prasad, A. C. Levitt, and D. A. Weitz, “Three-dimensional confocal microscopy of colloids,” *App. Optics* **40**, 4152–4159 (2001).
- [25] A. van Blaaderen and P. Wiltzius, “Real-space structure of colloidal hard-sphere glasses,” *Science* **270**, 1177–1179 (1995).
- [26] M. D. Ediger, C. A. Angell, and S. R. Nagel, “Supercooled liquids and glasses,” *J. Phys. Chem.* **100**, 13200–13212 (1996).
- [27] C. A. Angell, K. L. Ngai, G. B. McKenna, P. F. McMillan, and S. W. Martin, “Relaxation in glassforming liquids and amorphous solids,” *J. App. Phys.* **88**, 3113–3157 (2000).

- [28] W. van Meegen and P. N. Pusey, “Dynamic light-scattering study of the glass transition in a colloidal suspension,” *Phys. Rev. A* **43**, 5429–5441 (1991).
- [29] R. M. Ernst, S. R. Nagel, and G. S. Grest, “Search for a correlation length in a simulation of the glass transition,” *Phys. Rev. B* **43**, 8070–8080 (1991).
- [30] P. N. Pusey and W. van Meegen, “Phase behaviour of concentrated suspensions of nearly hard colloidal spheres,” *Nature* **320**, 340–342 (1986).
- [31] I. Snook, W. van Meegen, and P. Pusey, “Structure of colloidal glasses calculated by the molecular-dynamics method and measured by light scattering,” *Phys. Rev. A* **43**, 6900–6907 (1991).
- [32] R. L. Davidchack and B. B. Laird, “Simulation of the hard-sphere crystal–melt interface,” *J. Chem. Phys.* **108**, 9452–9462 (1998).
- [33] S. Auer and D. Frenkel, “Prediction of absolute crystal-nucleation rate in hard-sphere colloids,” *Nature* **409**, 1020–1023 (2001).
- [34] J. D. Bernal, “The Bakerian lecture, 1962. The structure of liquids,” *Proc. Roy. Soc. London. Series A* **280**, 299–322 (1964).
- [35] B. J. Alder and T. E. Wainwright, “Decay of the velocity autocorrelation function,” *Phys. Rev. A* **1**, 18–21 (1970).
- [36] J. Mittal, J. R. Errington, and T. M. Truskett, “Does confining the hard-sphere fluid between hard walls change its average properties?” *J. Chem. Phys.* **126**, 244708 (2007).
- [37] Z. T. Németh and H. Löwen, “Freezing and glass transition of hard spheres in cavities,” *Phys. Rev. E* **59**, 6824–6829 (1999).
- [38] B. Doliwa and A. Heuer, “Cage effect, local anisotropies, and dynamic heterogeneities at the glass transition: A computer study of hard spheres,” *Phys. Rev. Lett.* **80**, 4915–4918 (1998).
- [39] R. J. Speedy, “The hard sphere glass transition,” *Molecular Physics* **95**, 169–178 (1998).
- [40] J. D. Weeks, D. Chandler, and H. C. Andersen, “Role of repulsive forces in determining the equilibrium structure of simple liquids,” *J. Chem. Phys.* **54**, 5237–5247 (1971).
- [41] P. M. Chaikin, “Thermodynamics and hydrodynamics of hard spheres; the role of gravity,” in M. E. Cates and M. R. Evans, eds., “Soft and Fragile Matter, Nonequilibrium Dynamics, Metastability and Flow,” pages 315–348 (Institute of Physics, London) (2000).
- [42] S. Torquato, T. M. Truskett, and P. G. Debenedetti, “Is random close packing of spheres well defined?” *Phys. Rev. Lett.* **84**, 2064–2067 (2000).
- [43] C. S. O’Hern, L. E. Silbert, A. J. Liu, and S. R. Nagel, “Jamming at zero temperature and zero applied stress: The epitome of disorder,” *Phys. Rev. E* **68**, 011306 (2003).

- [44] A. Donev, S. Torquato, F. H. Stillinger, and R. Connelly, “Comment on ‘jamming at zero temperature and zero applied stress: The epitome of disorder’,” *Phys. Rev. E* **70**, 043301 (2004).
- [45] C. S. O’Hern, L. E. Silbert, A. J. Liu, and S. R. Nagel, “Reply to ‘Comment on “Jamming at zero temperature and zero applied stress: The epitome of disorder” ’,” *Phys. Rev. E* **70**, 043302 (2004).
- [46] A. Van Blaaderen, A. Imhof, W. Hage, and A. Vrij, “Three-dimensional imaging of submicrometer colloidal particles in concentrated suspensions using confocal scanning laser microscopy,” *Langmuir* **8**, 1514–1517 (1992).
- [47] H. Yoshida, K. Ito, and N. Ise, “Localized ordered structure in polymer latex suspensions as studied by a confocal laser scanning microscope,” *Phys. Rev. B* **44**, 435–438 (1991).
- [48] M. Elliot, B. Bristol, and W. Poon, “Direct measurement of stacking disorder in hard-sphere colloidal crystals,” *Physica A* **235**, 216–223 (1997).
- [49] J. Brujic, C. Song, P. Wang, C. Briscoe, G. Marty, and H. A. Makse, “Measuring the coordination number and entropy of a 3d jammed emulsion packing by confocal microscopy,” *Phys. Rev. Lett.* **98**, 248001 (2007).
- [50] J. Zhou, S. Long, Q. Wang, and A. D. Dinsmore, “Measurement of forces inside a three-dimensional pile of frictionless droplets,” *Science* **312**, 1631–1633 (2006).
- [51] E. R. Weeks and D. A. Weitz, “Properties of cage rearrangements observed near the colloidal glass transition,” *Phys. Rev. Lett.* **89**, 095704 (2002).
- [52] E. R. Weeks, J. C. Crocker, A. C. Levitt, A. Schofield, and D. A. Weitz, “Three-dimensional direct imaging of structural relaxation near the colloidal glass transition,” *Science* **287**, 627–631 (2000).
- [53] W. K. Kegel and A. van Blaaderen, “Direct observation of dynamical heterogeneities in colloidal hard-sphere suspensions,” *Science* **287**, 290–293 (2000).
- [54] M. D. Ediger, “Spatially heterogeneous dynamics in supercooled liquids.” *Annu. Rev. Phys. Chem.* **51**, 99–128 (2000).
- [55] A. Kasper, E. Bartsch, and H. Sillescu, “Self-diffusion in concentrated colloid suspensions studied by digital video microscopy of core-shell tracer particles,” *Langmuir* **14**, 5004–5010 (1998).
- [56] A. H. Marcus, J. Schofield, and S. A. Rice, “Experimental observations of non-Gaussian behavior and stringlike cooperative dynamics in concentrated quasi-two-dimensional colloidal liquids,” *Phys. Rev. E* **60**, 5725–5736 (1999).
- [57] T. G. Mason and D. A. Weitz, “Optical measurements of frequency-dependent linear viscoelastic moduli of complex fluids,” *Phys. Rev. Lett.* **74**, 1250–1253 (1995).

- [58] T. G. Mason, K. Ganesan, J. H. van Zanten, D. Wirtz, and S. C. Kuo, “Particle tracking microrheology of complex fluids,” *Phys. Rev. Lett.* **79**, 3282–3285 (1997).
- [59] T. A. Waigh, “Microrheology of complex fluids,” *Rep. Prog. Phys.* **68**, 685–742 (2005).
- [60] V. Breedveld and D. J. Pine, “Microrheology as a tool for high-throughput screening,” *Journal of Materials Science* **38**, 4461–4470 (2003).
- [61] R. G. Larson, *The Structure and Rheology of Complex Fluids* (Oxford University Press, USA) (1998), ISBN 019512197X.
- [62] J. C. Crocker, M. T. Valentine, E. R. Weeks, T. Gisler, P. D. Kaplan, A. G. Yodh, and D. A. Weitz, “Two-point microrheology of inhomogeneous soft materials,” *Phys. Rev. Lett.* **85**, 888–891 (2000).
- [63] A. J. Levine and T. C. Lubensky, “Two-point microrheology and the electrostatic analogy,” *Phys. Rev. E* **65**, 011501 (2001).
- [64] D. T. Chen, E. R. Weeks, J. C. Crocker, M. F. Islam, R. Verma, J. Gruber, A. J. Levine, T. C. Lubensky, and A. G. Yodh, “Rheological microscopy: Local mechanical properties from microrheology,” *Phys. Rev. Lett.* **90**, 108301 (2003).
- [65] D. J. Tritton, *Physical Fluid Dynamics* (Oxford Science Publications) (Oxford University Press, USA), 2 edition (1988), ISBN 0198544936.
- [66] M. Frank, D. Anderson, E. R. Weeks, and J. F. Morris, “Particle migration in pressure-driven flow of a Brownian suspension,” *J. Fluid Mech* **493**, 363–378 (2003).
- [67] C. Gao, B. Xu, and J. F. Gilchrist, “Mixing and segregation of microspheres in microchannel flows of mono- and bidispersed suspensions,” *Phys. Rev. E* **79**, 036311 (2009).
- [68] S. A. Koehler, S. Hilgenfeldt, E. R. Weeks, and H. A. Stone, “Drainage of single plateau borders: Direct observation of rigid and mobile interfaces,” *Phys. Rev. E* **66**, 040601 (2002).
- [69] S. A. Koehler, S. Hilgenfeldt, E. R. Weeks, and H. A. Stone, “Foam drainage on the microscale II. imaging flow through single plateau borders,” *J. Colloid Interf. Sci.* **276**, 439–449 (2004).